

1 **Supplementary Material**

2

3 Graphene-Silver Hybrid Nanoparticles Embedded Phase  
4 Change Materials for Enhanced Thermal Management of  
5 Lithium-Ion Batteries

6

7

8 *Balan Akshay<sup>1</sup>, Faisal Seyas Seyas Mumthas<sup>1</sup>, Manu Mohan<sup>1</sup>, Vishnu Bhuvanachandran*  
9 *Rajeswari<sup>1†</sup> and C. Ravikumar<sup>2\*</sup>*

10

11 <sup>1</sup> *Energy Research Lab, Department of Mechanical Engineering, Marian Engineering College,*  
12 *Kazhakuttom, Thiruvananthapuram - 695582, Kerala, India*

13

14 <sup>2</sup> *Department of Chemical Engineering, Indian Institute of Technology Dharwad, Dharwad -*  
15 *580 011, Karnataka, India*

16

17

18 \*C. Ravikumar (Corresponding Author)

19 Department of Chemical Engineering, Indian Institute of Technology Dharwad,  
20 Chikkamalligawad, Dharwad - 580 011, Karnataka, India

21 E-mail: ravikumar@iitdh.ac.in, ravikumarc2006@gmail.com

22 Phone: 91- 836 2309741

23

24

25 †Vishnu Bhuvanachandran Rajeswari (Co-Corresponding Author)

26 Department of Mechanical Engineering, Marian Engineering College,  
27 Thiruvananthapuram - 695582, Kerala, India

28 E-mail: vishnu@marian.ac.in

29 Phone: 91- 989 5575793

30

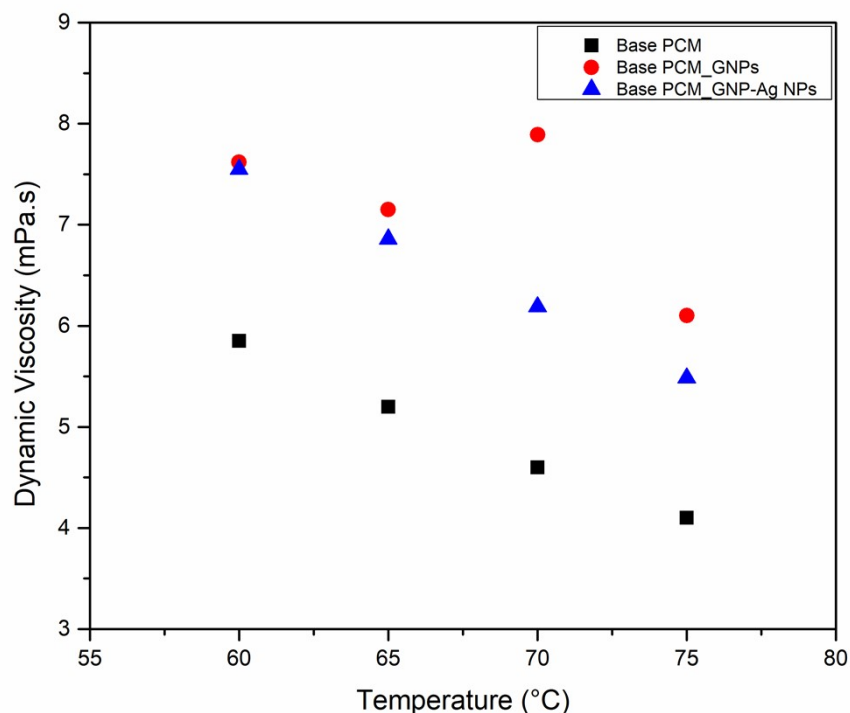
31 **1) Determination of thermophysical properties of PCM and NP-impregnated PCMs at**  
32 **a loading concentration of 0.1 wt%.**

33

34 **Average Density:** The weighted average densities of the base PCM, PCM-GNPs, and PCM-  
35 GNP-Ag NPs were calculated by utilizing the individual densities provided by the  
36 manufacturers for paraffin wax, stearic acid, silver, and GNPs. The weighted average densities  
37 for each of these compositions were calculated using the effective density model introduced by  
38 Yu et al. <sup>1</sup>.

39 **Dynamic viscosity:** The dynamic viscosity measurements of base PCM and those loaded with  
40 GNPs and GNP-Ag hybrid NPs were conducted using a Rheometer (Brookefield LVDV-III  
41 Ultra Cone Plate Rheometer, USA) to controlled temperature conditions within the range of  
42 60°C to 75°C, covering the phase transition temperature range of the PCM. The average  
43 viscosity values recorded between 60 to 70 °C are mentioned in Table 2 (of the main  
44 manuscript). The instrument employs the principle of rotational viscometry, where the torque  
45 required to rotate a cone spindle immersed in the sample is measured. It calculates the dynamic  
46 viscosity based on the applied torque and the rotational speed of the spindle. The accuracy of  
47 the viscosity values obtained using the Rheometer with Cone Spindle CPE-40 and a sample  
48 volume of 0.5 mL is within  $\pm 1\%$  of the Full Scale Range (FSR) recorded viscosity value,  
49 where FSR varies with cone spindle and rotational speed selection. The values reported are the  
50 average of multiple measurements taken at each temperature point, with a shear rate of  $7.5 \text{ s}^{-1}$ .

51 Analyzing the dynamic viscosity values across different temperatures reveals the temperature-  
52 dependent behavior of the PCM samples. Comparing the dynamic viscosity of the PCM with  
53 those loaded with GNPs and GNP-Ag hybrid NPs highlights the influence of NP addition on  
54 the increase in the viscosity as shown in Fig.S1, indicating potential alterations in the fluid  
55 dynamics and rheological properties of the PCM mixtures.



56

57 **Fig. S1.** Measured dynamic viscosity values of base PCM, and PCMs loaded with 0.1 % GNPs and  
 58 GNP-Ag hybrid NPs at different temperatures.

59

60 Across all PCM variants, a consistent decrease in dynamic viscosity with increasing  
 61 temperature was observed. Interestingly, while both GNPs and GNP-Ag hybrid NPs led to  
 62 increased viscosity compared to the base PCM, the magnitude of this effect varied between the  
 63 two nanoparticle types. Specifically, at 70°C, PCM-GNPs exhibited a higher dynamic viscosity  
 64 than PCM-GNP-Ag NPs due to the potential influence of aggregate GNP morphology and  
 65 composition on viscosity behavior.

66

67 **Thermal Conductivity:** The TPS 500 S instrument employs the transient planar source  
 68 method for thermal conductivity measurements, generating a brief heat pulse within the Kapton  
 69 sensor via Joule heating. The measurement process utilized parameters such as an initial  
 70 temperature of 33°C, an output power of 25 mW, a measurement time of 5 s, a radius of 3.189  
 71 mm, and a thermal coefficient of resistance (TCR) of 0.004930 K<sup>-1</sup>. These parameters were  
 72 crucial for accurately determining the thermal conductivity of the sample. As the pulse

73 traverses through the sensor and into the sample material, it induces temperature changes,  
74 measured by temperature sensors embedded in the Kapton sensor. The thermal conductivity of  
75 the sample under study was determined with an accuracy better than 5%. This measured  
76 thermal conductivity value is a critical indicator of the material's heat transfer characteristics.

77 The base PCM's thermal conductivity is recorded to be  $0.270 \text{ W}\cdot\text{m}^{-1}\text{K}^{-1}$ . Incorporating 0.1 wt%  
78 GNPs increases this to  $0.301 \text{ W}\cdot\text{m}^{-1}\text{K}^{-1}$ , while adding 0.1 wt% GNP-Ag hybrid NPs further  
79 enhances it to  $0.325 \text{ W}\cdot\text{m}^{-1}\text{K}^{-1}$ . These reference values represent distinct compositions and  
80 illustrate the effect of additives on improving thermal conductivity. GNPs, for instance, are  
81 known for their high thermal conductivity; when added to the PCM, they enhance their thermal  
82 conductivity. Similarly, Ag NPs possess excellent thermal conductivity properties, and when  
83 combined with GNPs, they further boost the material's ability to conduct heat. These additives  
84 create pathways for more efficient heat transfer within the material, thus resulting in higher  
85 overall thermal conductivity values.

86 **Specific heat capacity and latent heat of solidification:** Specific heat capacities (liquid and  
87 solid) and latent heat of solidification of all the samples were calculated using the T-history  
88 method as described by Radhakrishnan and Sobhan <sup>2</sup>. The calculated base PCM-specific heat  
89 capacity values are  $2.16 \text{ J}\cdot\text{g}^{-1}\text{K}^{-1}$  and  $5.01 \text{ J}\cdot\text{g}^{-1}\text{K}^{-1}$  for liquid and solid, respectively. By  
90 incorporating 0.1 wt% GNP these values increased to  $2.64 \text{ J}\cdot\text{g}^{-1}\text{K}^{-1}$  and  $5.14 \text{ J}\cdot\text{g}^{-1}\text{K}^{-1}$ ,  
91 respectively. Further for 0.1 wt% GNP-Ag hybrid NPs, the values increased to  $2.43 \text{ J}\cdot\text{g}^{-1}\text{K}^{-1}$   
92 and  $5.56 \text{ J}\cdot\text{g}^{-1}\text{K}^{-1}$  for the corresponding liquid and solid phases. The improvements observed  
93 are attributed to the increased surface area offered by the NPs within the PCM matrix. This  
94 enhanced surface area fostered efficient heat transfer processes due to stronger PCM molecules  
95 and NPs interactions. Consequently, thermal conductivity is improved, leading to higher  
96 specific heat capacities in both liquid and solid phases. Additionally, the calculated latent heat  
97 of solidification for the base PCM was determined to be  $147 \text{ J}\cdot\text{g}^{-1}$ . However, with the inclusion

98 of 0.1 wt% GNP and GNP-Ag hybrid NPs, this value decreased to 140 J.g<sup>-1</sup> and 144 J.g<sup>-1</sup>,  
99 respectively. This reduction is beneficial for enhancing the thermal performance of PCMs.

100

## 101 **References**

- 102 1 W. Yu, D. M. France, S. Choi and J. L. Routbort, *OSTI OAI (U.S. Department of Energy*  
103 *Office of Scientific and Technical Information)*, DOI:<https://doi.org/10.2172/919327>.
- 104 2 N. Radhakrishnan and C. B. Sobhan, *Heat and Mass Transfer*, 2022, **58**, 1811–1828.